



فصلنامه مدیریت شهری
(ضمیمه لاتین)

Urban management

No.44 Autumn 2016

■ 113 - 122 ■

Received 23 Mar 2015; Accepted 11 June 2016

A flood risk projection for Soleimantangeh Dam against future climate change

Amir Khosrojerdi - *Water Engineering Department, Science and research Branch, Islamic Azad University, Tebran, Iran.*

Mostafa Fallah¹ - *Graduated in Water Engineering, Science and research Branch, Islamic Azad University, Tebran, Iran.*

Abstract

A sensitivity analysis of the flood safety of Solaimantangeh dam using a regional climate change simulation is presented. Based on the output of the CCSM (Community Climate Change System Model) general circulation model, the NIRCM (North of Iran Regional Climate Model) computes regional scale output with 50 km spatial resolution and 21 vertical layers. Using the SRES (Special Report Emission Scenario) “B1” Climate Change Scenario when applied to the Tajan river basin, where Solaimantangeh dam is located, NIRCM reduces significantly the bias in Annual Maximum Event total Precipitation (AMEP) & Annual Maximum Daily Precipitation (AMDP) that CCSM shows. The stream flow change scenario is then simulated using SSARR (Stream flow Synthesis and Reservoir Regulation) model. A rainfall-runoff model was implemented using precipitation and temperature projected by CCSM and NIRCM. The model demonstrated that average Stream flow would increase 38.7% and the variability would increase 14.3%. This remarkable increase in projected annual maximum flow for the next 20 years (2004-2023) should be a significant negative signal to water resources managers. The results indicate that the number of floods remains almost the same, but that the magnitude of a single flood event and the recovery from it become worse.

Key words: *Flood, Risk, Dam, climate change.*

1. Corresponding Author, Tel: 22141681, Email: Mostafafalh@gmail.com

1. Introduction

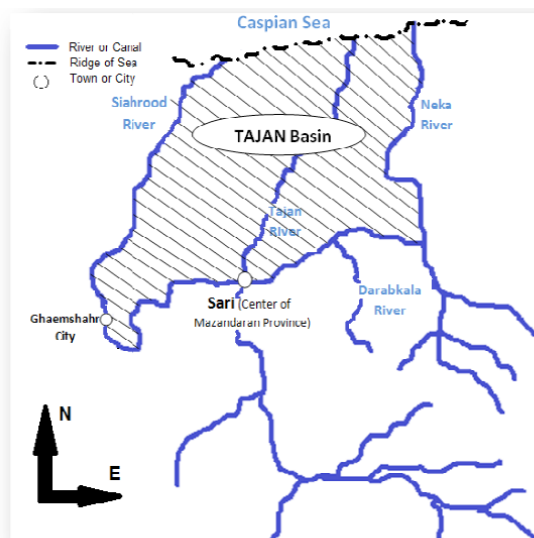
General Climate Models (GCMS) and their spatially downscaled versions, Regional Climate Models (RCMS), provide superb areal coverage. Hydrologists employ the outputs of the models to characterize the interaction between the land surface and the atmosphere and to assess the hydrological effects of climate change. While time series data are essential for assessing the hydrological effects of climate change on medium or small sized watersheds, time series of hydro-meteorological variables of interest such as precipitation (or rainfall) are not always available at the desired time interval. Therefore, hydro-meteorological data with time scales on the order of 1 h less are urgently required. There is consensus that the recent increase in frequency and magnitude of natural disasters such as flood, drought, and Asian sandy dust are closely related to climate change. Numerous climate change impact studies have been funded since 1990, but the precise impact of climate change on local water resources still remains uncertain. However, the results of those past studies show inconsistencies. Moreover, most of those studies were limited to stream flow change simulation, while the sensitivity of water resource systems to climate change was rarely addressed. This research

studies water resources systems issues, focusing on flood risk. As in other climate change impact studies, a series of hydrologic and atmospheric models was connected in one way. In this study, climate change scenarios that included an atmospheric doubling of CO₂ were generated from a General Circulation Model (GCM) and downscaled to an appropriate river basin scale with a regional climate model. These data saved as input to hydrologic model to generate climate impacted stream flows for a study basin. These were then used in a river basin simulation model to investigate the sensitivity of a reservoir system to climate change for flood risk.

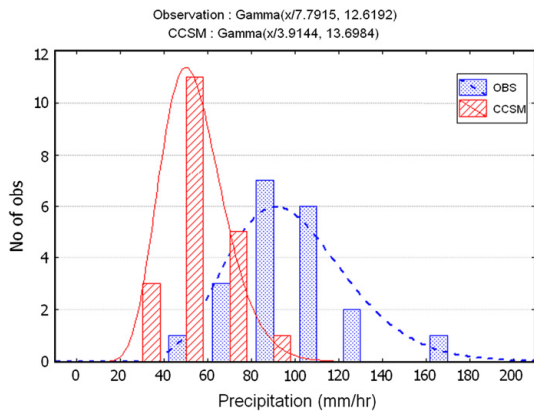
2. Research method

2.1 Case study

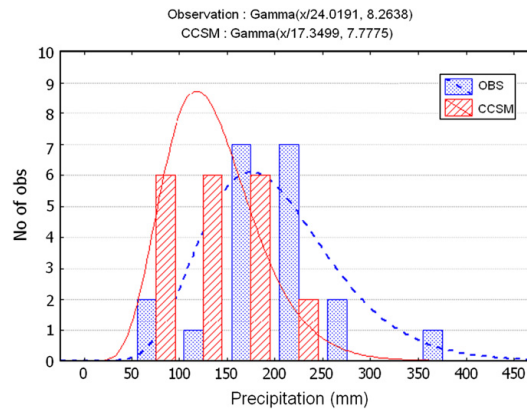
Tajan is an area in the North of Iran with about 460000 inhabitants and at least 60% of them work on farms. Cashing subsidies policy in this area, certainly effects on people in obviating their daily water needs. Tajan area is more than 90940 hectares. It is bounded from east to Neka River, west to Siyahrood River, North to Mazandaran Sea (Caspian Sea) and Sought to Alborz mountains. This system is in 53°15'to 53°53' of geographical longitude and 36°25'to 36°50' of latitude and is contained of some important cities such as Sari, center



▲ Fig 1. Map of Tajan



▲ Fig2. Statistical differences between CCSM – Simulated and observed AMDP (2004-2013).



▲ Fig3. Statistical differences between CCSM – Simulated and observed AMEP (2004-2013)

of Mazandaran province, Neka, one of the biggest center of electricity generation in Iran and Ghaemshahr, one of the most important commercial city in north of Iran (Fig. 1).

2.2 Community climate system model

The community climate system model (CCSM) is a GCM (global climate system) developed by cooperative agencies such as the US department of energy and the National Air and Space Administration, guided by the National Center for Atmospheric Research (NCAR) in Boulder Colorado, USA. Composed of four separate dynamical geophysical models, it simulates the earth's atmosphere, ocean, land surface and sea-ice, and one central coupler component simultaneously. It is well known that GCMs tend to underestimate areal precipitation. To examine whether CCSM also has this tendency, a simulated set of precipitation data from 2004 to 2013 at CCSM grid points was converted to a real mean precipitation for the Solaimantangeh basin and compared with observed precipitation for the same period. The reference scenario is produced by GCM assuming current climate conditions such as CO₂ concentration and land use patterns. Of interest are statistical differences between the simulated and observed series rather than a daily one to one comparison between them. Fig. 2 and 3 show these differences for annual maximum event total precipitation (AMEP) and annual maximum daily precipitation

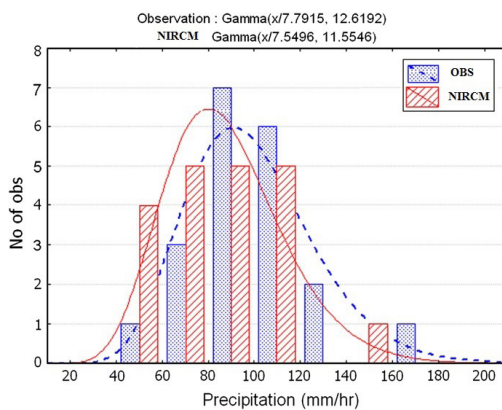
(AMDP). On average, simulated AMEP is 32% less than observed one and simulated AMDP is 45.5% less than observed one when both data sets are fitted with gamma distributions (Table2).

2.3 Regional Climate Model (RCM)

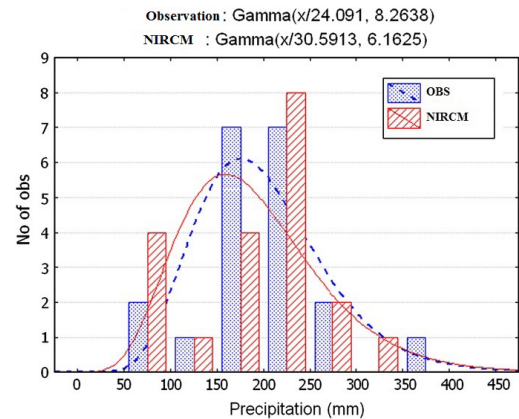
This study utilizes a regional climate model (RCM) called NIRCM to downscale CCSM because its performance has been well verified by other similar studies. NIRCM couples a meso scale numerical prediction model (PSU/NCAR MM5) that uses a non-static equations system with a complex terrain model (NCAR/LSM) to improve RCM2 of NCAR. While RCM2 has a limitation in simulating local weather in areas less than 10 km on the spatial lateral grid scale, this model can be used for mountainous areas with land surface characteristics that are typical in North of Iran because its dynamic physical procedure can be applied to the spatial scale over less than a few kilometers without modification. In this study, NIRCM implements regional simulations using the output produced by CCSM under a nested grid system with 60 km resolution. It is expected that regionalization or downscaling through RCM could efficiently reduce the underestimation tendency of CCSM mentioned previously. Figs. 4 and 5 shows the statistical characterization of NIRCM simulated AMEP and AMDP from 2004 to 2013. NIRCM simulated AMEP is 5.3 % less than the corresponding observation,

Model		(α)	(β)	Mean (= $\alpha\beta$)	Standard Deviation (= $\alpha\beta^{1/2}$) (mm)	
CCSM	Annual Max.	Observation	12.62	7.79	98.31	35.22
	Daily Precipitation	Simulation	13.7	3.91	53.57	27.09
	Annual Max.	Observation	8.26	24.02	198.4	40.48
	Event Total Precipitation	Simulation	7.78	17.35	134.9	32.41
NIRCM	Annual Max.	Observation	12.66	7.79	98.31	35.22
	Daily Precipitation	Simulation	11.55	7.55	87.2	31.74
	Annual Max Event	Observation	8.26	24.09	198.9	40.54
	Total Precipitation	Simulation	6.16	30.59	188.4	34.07

▲ Table1. Gamma distribution parameters and basic statistics of CCSM- and NIRCM-simulated AMDP & AMEP



▲ Fig4. Statistical differences between NIRCM-simulated and observed AMDP (2004-2013).



▲ Fig 5. Statistical differences between NIRCM-simulated and observed AMEP (2004-2013).

and simulated AMDP is 11.3% less (Table 2).

2.4 Stream flow simulation under climate change

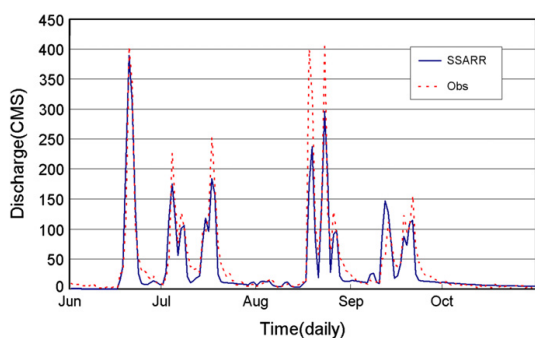
2.4.1 Continuous rainfall-runoff modeling: SSARR

The stream flow synthesis and reservoir regulation (SSARR) model was developed by the U.S Army Corps of Engineers in 1956 to provide mathematical, hydrological simulations required for the planning, design, and operation of water control works. Available in the public domain, SSARR has been widely used for operational river forecasting and management in many countries, including

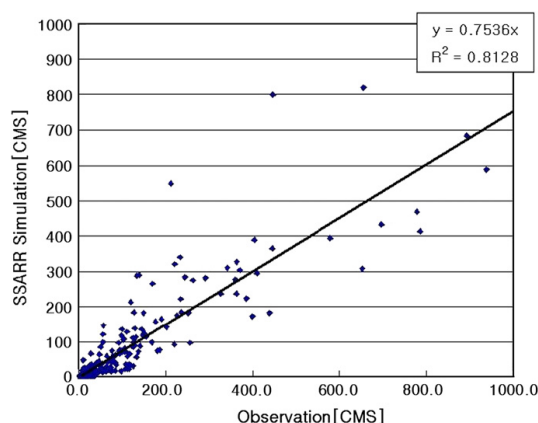
Iran. SSARR consists of two major modules: the watershed model and the river system and reservoir regulation model. Stream flows throughout the basin can be synthesized by simulating the effects of channel routing, diversions, reservoir regulation and storage. More than 24 parameters including SMI (soil moisture index), ETI (evapotranspiration index), BII (base flow infiltration index) should be calibrated, and incremental time units can be selected for 6 minutes to 24 hours. Like other hydrologic models, SSARR has a unique algorithm for subtracting loss from total precipitation, estimating direct runoff

and base flow, and computing surface runoff and interflow. When precipitation occurs the model identifies it as rainfall or snow. The snow contributes to stream flow according to the snow melting process. The rainfall flows partly to direct runoff and the remaining to the increase of soil moisture which is represented by the SMI (soil moisture index), and others to evapotranspiration. Total runoff is separated into direct runoff and the base flow using BII (base flow infiltration index). Direct runoff contributes to surface runoff and interflow using S-SS (surface and subsurface), while base flow goes to groundwater flow and groundwater return flow. Those four stream flow components are calculated individually and eventually become inflow to main stream channels. The basic watershed and channel routing scheme employed in the SSARR model is the cascade of reservoir, which is similar to the Nash model wherein the long and attenuation of the flood wave are simulated through successive increments of lake type storage. The SSARR model has two complete watershed models: the integrated – snow band model, which is applied in this study, and the Depletion curve model. The parameter set for the integrated – snow band model consists of physical, hydro meteorological and internal parameters. Physical parameters refer to sub basin delineation, Thiess coefficient, and

areal ratio by topographical elevation, and reservoir characterization on release from the dam. Hydro meteorological parameters are basin weighted average precipitation PP, basin weighted average temperature TA, evapotranspiration index ETI, basin weighted potential evapotranspiration ETP, snow band potential evapotranspiration PET, monthly adjustment factor for evapotranspiration ETMO, elevation adjustment factor ETEL, soil moisture adjustment factor DKE, and adjustment to PET for rainfall intensity EKE. Internal parameters include runoff percent ROP for SMI, total base flow percent BFP for SMI, storage time BIITS for calculation of BII, maximum value of BII (BIIMAX), minimum input rate to base flow and lower zone routing components, and percent of total base flow going to lower zone routing PBLZ. The most sensitive of the internal parameters are SMI-ROP, BII-BFP, and S-SS. The effects of other parameters on runoff are relatively insignificant. The daily stream flow scenarios can be produced by coordinating the GCM, the regional atmospheric model, and the rainfall – runoff model. The stream flow scenarios depend on the climate change scenarios. However, one climate change scenario can produce different stream flow because there are sub-grid scale variability in precipitation and temperature, etc. Fig.6 shows that peak



▲ Fig6. SSARR simulated and observed Stream flow time series in 2013.



▲ Fig7. Scatterplot of SSARR simulated and observed Stream flow time series in 2013

	PAST (2004-2014)	FUTURE (2015-2025)	CHANGE %
Average	20.8	28.85	38.7
Standard Deviation	52.4	83.12	58.6
Coefficient of Variation	2.52	2.88	14.3
Std. Skewness	176.67	206.3	16.8
Std. Kurtosis	805.76	1245.3	54.5
Min (CMS)	1.33	1.97	48.1
Max (CMS)	748.68	1679.16	124.3

▲Table3. Basic statistics of simulated Stream flow for past and future.

flood simulated with SSARR tends to be underestimated, but the peak time and overall pattern follow the observation ones reasonably well. Fig.7 presents a regression of the SSARR simulation with observed value from 2004 and 2013, yielding $R^2 = 0.81$ which is moderately high.

2.4.2 Stream flow change scenarios

This study uses the SRES (special report on emission scenarios) B1 scenario of CCSM. Among 4 scenario groups prepared by SRES (A1, A2, B1, and B2), the B1 scenario assumes a convergent world with low population growth as in A1, but with rapid changes in economic structure (IPCC, 2000). We simulated a stream flow change scenario with SSARR using the NIRCM precipitation scenario for the period from 2004 to 2013. We then compared two sets of simulated stream flow series, one from past (2004-2013) and the other from future (2014-2023) with respect to their key statistics (Table 3). Mean and maximum stream flows increase 38.7% and 124.3%, respectively, although the coefficient of variation increases only 14.3%. Fig.8 shows the ordered comparison between past and future for annual simulated stream flow and projects a relatively large increase in the annual maximum, warning of flood risk in the future.

2.4.3 Impact of climate change on flood risk

Analysis of sensitivity to climate change or a spill from the Solaimantangeh dam reservoir was carried out to assess system safety against

flood risk. A spill is defined as release greater than the maximum release for hydropower generation when the reservoir elevation reaches its maximum. Sensitivity is measured using the performance criteria of a water resources system such as reliability, resiliency, and vulnerability. Reliability is defined as the percentage of time that the system operates without failure. For a certain period t , if the system's output for a certain variable X_t is satisfactory, the state during time t is defined as S ; otherwise the state is defined as F . The system's reliability is defined as:

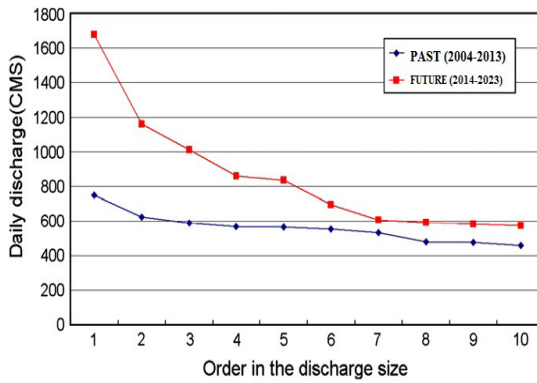
$$\alpha = P_r(X_t \in S)$$

The risk can be simply defined as $1 - \alpha$. Resiliency is defined as the ability of the system to recover ones failure has occurred. The resiliency ρ of a system can be considered in the planning horizon as follows:

$$\rho = (P_r(X_{t+1} \in S | P_r(X_t \in F))$$

Resiliency is basically a measure of the duration of an unsatisfactory condition. This indicator is important in drought and flood conditions because the damage and costs associated with both are greatly affected by the duration of unsatisfactory operations. Vulnerability is defined as the average magnitude of failures. Reliability and resiliency range from 0 to 1 and vulnerability is positive but unlimited. It is defined as:

$$v = \frac{\sum_{t=1}^n Q_t}{N_F}$$



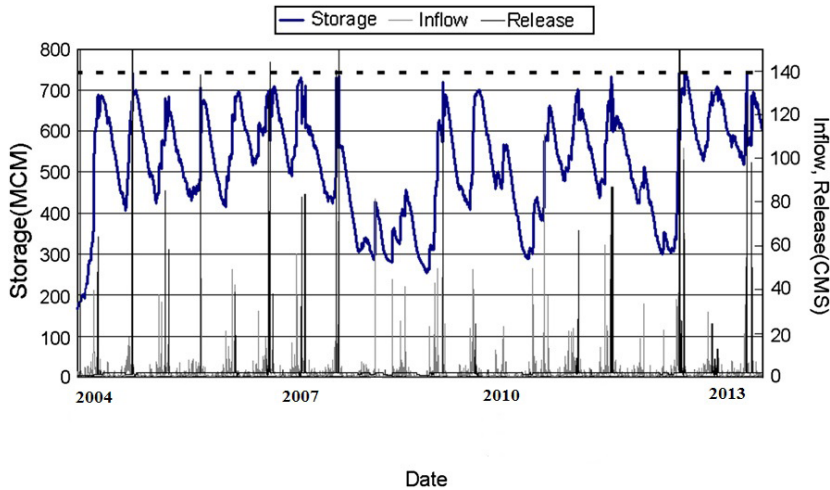
▲ Fig8. Ordered comparison between PAST and FUTURE for annual Streamflow simulation using NIRCM

Where Q_t is the magnitude of failure during time t . the higher reliability and resiliency are, and the smaller vulnerability is, the better the system performs. Since this study is interested in flood risk, these criteria were calculated with respect to a spill that occurs when water availability exceeds the storage capacity of Solaimantangeh dam, which becomes:

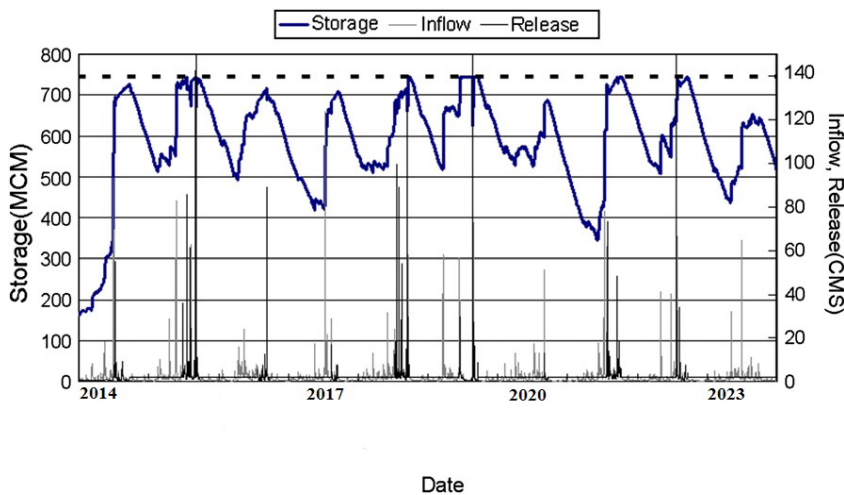
Reliability = $1 - (\text{number of days where spill occurs}) / (\text{total number of days})$

Resiliency = $(\text{number of days when the system goes into failure}) / (\text{number of days when spill occurs})$

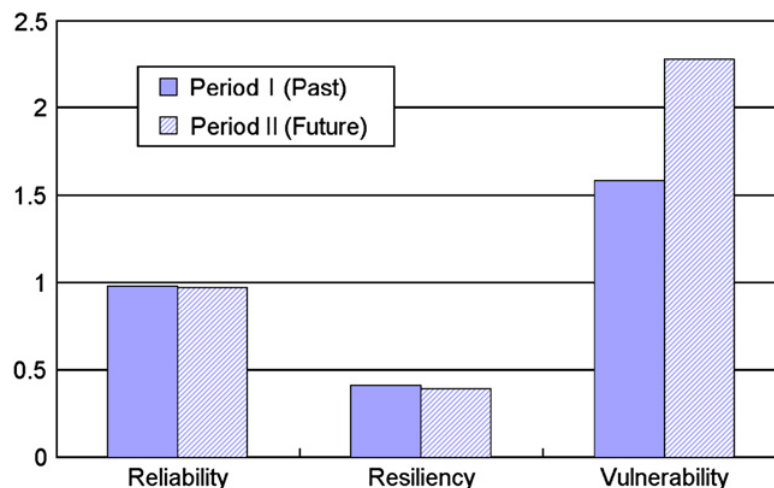
Vulnerability = $(\text{total number of spills}) / (\text{number of days when spill occurs})$.



▲ Fig9. The storage (MCM), inflow (CMS) and outflow (CMS) during the past period.



▲ Fig10. The storage (MCM), inflow (CMS) and outflow (CMS) during the future period.



▲ Fig11. Sensitivity analysis results for Solaimantangeh dam.

3. Result

As in Table 2, the simulation period is divided into 2 periods: past (2004 – 2013) and future (2014 – 2023). Fig.9 shows storage vs. inflow and release for the past period, and Fig.10 shows the same plot for the future period.

In Figs. 9 and 10, initial storage was defined as 164.33 MCM which is the actual storage in Solaimantangeh dam from January 2004. Reliability, resiliency, and vulnerability are calculated when storage meets the dashed line which represents 742.5 MCM, the maximum storage of Solaimantangeh Dam. Results of the simulation for Solaimantangeh Dam are shown in Fig.11. All criteria become worse for future values than for past values. Even though future reliability is slightly increased, the resiliency is decreased 21.6 % and vulnerability is increased 35.6%. In other words, it is likely that the total number of flood events remains almost the same, but the magnitude and recovery from a single event become worse.

Conclusion

To overcome this increased flood potential, the water managers for Solaimantangeh Dam may need to seriously consider a modification of the current operating rule. Due to the warming climate, increased moisture evaporated contributes to precipitation increases in the mid-latitude regions. Calculation of dam discharge using the SSARR based on precipitation and

temperature projected by CCSM and NIRCM for the climate change scenario B1 shows an increase of 38.7 % in average stream flow, and the vulnerability increases 14.3%. This could lead to deterioration of the current flood risk management system. In particular, the remarkable increase in annual maximum flow for the next 20 years (2004-2023) may be a notable detriment to water resources. We verified that the future safety index will be weakened compared to the past safety index.

References

- Bernell L. (1958). *Determination of Pressures in Earth Dams During Construction.*, 6th International Congress on Large Dams, New York, Report 117, volume III, pp373-384.
- Bernell L. (1982). *Experiences of Wet Compacted Dams In Sweden.*, Proc.14th International Congress on Large Dams, Rio de Janeiro, Vol.4, Q55/R24, pp 421-431.
- Dixon, Hugh H., M. A., M. I. C. E., M. ASCE. (1958). "Moisture Control and Compaction Methods Used During Construction of the Sasumua Dam, Kenya", 6th International Congress on Large Dams, New York, Question No.22, R. 12, pp 139-152.
- Kawakami, Fusaoshi, (1988). "Compaction Methods and Field Moisture Content of the Earth Core for Earth Dam Using the Mist Materials.", 6th International Congress on Large Dams, New York, Question No. 22, R. 28, Volume III, pp 165-183.
- Penman A. D, M. (1982). *General Report, Ques-*

tion 55: "Materials and Construction Methods for Embankment dams and cofferdams", Proc. 14th International Congress on Large Dams, Rio de Janeiro, Vol.4, pp.1105-1228.

Sherard, J. L., Woodward, R. j., Gizzienski, S. F. & Clevenger, W. A. (1963). *Earth & Earth-Rock Dams*. Wiley.

Takahashi M., Nakayama K. (1973). "The Effect of Regional Condition in Japan on Design and Construction of Impervious Elements of Rockfill Dams", 11th International Congress on Large Dams, Madrid, Report 29, Volume III, pp 501-524.

مدیریت شهری

فصلنامه مدیریت شهری
(ضمیمه لاتین)

Urban Management
No.44 Autumn 2016

■ 121 ■

مدیریت شهری

فصلنامه مدیریت شهری
(ضمیمه لاتین)

Urban Management
No.44 Autumn 2016

■ 122 ■